

# STRUCTURAL AND SUPERPARAMAGNETIC PROPERTIES OF ALUMINUM DOPED HAUSMANNITE NANOPARTICLES

\*<sup>1</sup> S. Karpagavalli, <sup>2</sup>S. John Kennady Vethanathan, <sup>3</sup>S. Perumal, <sup>4</sup>D. Priscilla Koilpillai and <sup>5</sup>A. Suganthi  
<sup>1</sup>Assistant Professor, <sup>2&3</sup> Principal, <sup>4&5</sup>Assistant Professor  
<sup>1&5</sup> Department of physics, Govindammal Aditanar College for women, Tiruchendur, Tamilnadu, India  
<sup>2&4</sup> Department of physics, St. John's College, Palayamkottai, Tamilnadu, India  
<sup>3</sup> Noorul Islam College of Arts and Science, Kumaracoil, Tamilnadu, India  
Affiliated to Manonmaniam sundaranar University, Abishekapatti, Tirunelveli, 627012, Tamilnadu, India

## ABSTRACT

Aluminum doped hausmannite ( $Mn_3O_4$ ) nanoparticles are synthesized by microwave assisted solvothermal method. The structural characteristics of as-synthesized aluminum doped  $Mn_3O_4$  nanoparticles are examined by powder X-ray diffraction technique (XRD). Fourier transform infrared (FTIR) method is used to confirm manganese, oxygen and aluminum exist in the sample. The SEM, FESEM and TEM pictures exhibits morphological properties of Al doped  $Mn_3O_4$  nanoparticles and calculated particle size to be in the range of 15 to 25 nm. The magnetic properties of aluminum doped  $Mn_3O_4$  nanoparticles are investigated by vibrating sample magnetometer (VSM).

**Key words:** Solvothermal, XRD, FTIR, SEM, FESEM and Magnetic studies

## 1 INTRODUCTION

Materials reduced to the nanoscale can show different properties compared to what they exhibit on a macroscale, enabling unique applications. Manganese oxides have attracted considerable interests due to their potential applications in many fields. As a mixed valent transition metal oxide,  $Mn_3O_4$  is particularly important. Decreasing particle size and doping elements are the effective way to improve the magnetic properties of the metal oxides. Recently, reported  $Mn_3O_4$  nanoparticles show relatively and higher coercive fields at low temperatures [1]. Moreover, Aluminum ( $Al^{3+}$ ) is considering as very good dopant in Li-ion batteries cathode material [2, 3]. Yu [4] and coworkers used a simple hydrothermal method to synthesis aluminum doped  $MnO_2$  nanoparticles and examine the electrochemical performance. Guiling Wang [5] coworkers prepare aluminum doped bulk manganese oxide nanoparticles using simple liquid-phase method and analyze electrochemical properties. In the solvothermal method, metal complexes are decomposed thermally, control particle size growth and limit agglomeration.

In this present work, Aluminum (2, 4, 6 and 8%) doped  $Mn_3O_4$  nanoparticles were synthesized by microwave assisted solvothermal method. Structural, morphological and magnetic properties of aluminum doped  $Mn_3O_4$  nanoparticles are examined by powder XRD, FTIR, SEM/ FESEM, TEM, EDAX and VSM.

## 2 EXPERIMENTAL DETAILS

### 2.1 Synthesis of Aluminum doped Manganese oxide nanoparticles

The Aluminum doped Manganese oxide nanoparticles  $Mn_3O_4$ : Al (2, 4, 6 and 8%) are synthesized by microwave assisted solvothermal method. All the reagents are of analytical grade and used without further purification. AR grade Manganese acetate tetrahydrate ( $Mn(CH_3COO)_2 \cdot 4H_2O$ ), Aluminum acetate dihydrate ( $Al(CH_3COO)_2 \cdot 2H_2O$ ) and Urea ( $H_2NCONH_2$ ) are used as precursors dissolved in 100 ml ethylene glycol ( $C_2H_6O_2$ ). Before the addition of aluminum acetate dihydrate, it was dissolved by adding few drops of NaOH solution in a proper manner. The mixed homogeneous solution is stirred well using magnetic stirrer for 2 hour. The microwave irradiation is carried out till the solvent evaporates completely. The prepared precipitates are washed with double distilled water two times and with acetone to remove unwanted organic impurities. The synthesized product are filtered and dried in an oven at  $50^\circ C$ . The doped samples annealing to a high temperature  $400^\circ C$  [6] in a muffle furnace for 1 hour, to obtain Aluminum doped  $Mn_3O_4$  nanoparticles.

### 2.2 Characterization

The structural characterization of as-prepared samples are examined by the use of powder X-ray diffraction (XRD) (Bruker AXS D8 Advance model diffractometer) using  $CuK_\alpha$ ,  $\lambda = 0.15406$  nm radiation. The functional groups present in the material were examined by Fourier Transform Infrared spectroscopy (FTIR) (SHIMADZU MODEL-IR AFFINITY-1) in the wavenumber range  $400 - 4000$   $cm^{-1}$ . The morphology of the as-prepared sample is tested by scanning electron microscope (SEM)

(JEOL Model JSM-6390LV) and field emission scanning electron microscope (FESEM) (SUPRA 55VP, Gemini Column, with air lock). Purity of all the doped samples are examined by Energy dispersive X-ray analysis (EDAX) by using Oxford Instruments X-MAX (20 mm<sup>2</sup>). Magnetic study was carryout by using vibrating sample magnetometer (VSM) (Model: Lake Shore 7410).

### 3. RESULTS AND DISCUSSIONS

#### 3.1 Structural characterization of Al doped Mn<sub>3</sub>O<sub>4</sub> by powder XRD analysis

Crystal phase and crystallinity of the as-synthesized nanoparticles were examined by powder X-ray diffraction analysis. The strong and sharp peaks indicate that they are without amorphous or crystalline. The powder XRD pattern exhibits the existence of tetragonal Mn<sub>3</sub>O<sub>4</sub>. Due to the calcination of the prepared samples, secondary phases are not detected. The significant XRD peaks can be well assigned to the crystal planes (211), (202), (220), (213), (004), (303), (224), (501), (404) and (503) with a hausmannite structure (JCPDS 75\_1560). The intensity of diffraction peak becomes weaker at low doping amount (2, 4% of Al) while becomes stronger when highly doped which indicate the amount of aluminum has influence on the structure of the final product [7]. There are no diffraction peak originating from aluminum in the XRD spectra. Fig 1 indicates the XRD pattern of Al doped Mn<sub>3</sub>O<sub>4</sub> nanoparticles. Fig 2 shows the Williamson-Hall plot for the prepared Al doped Mn<sub>3</sub>O<sub>4</sub> nano particles.

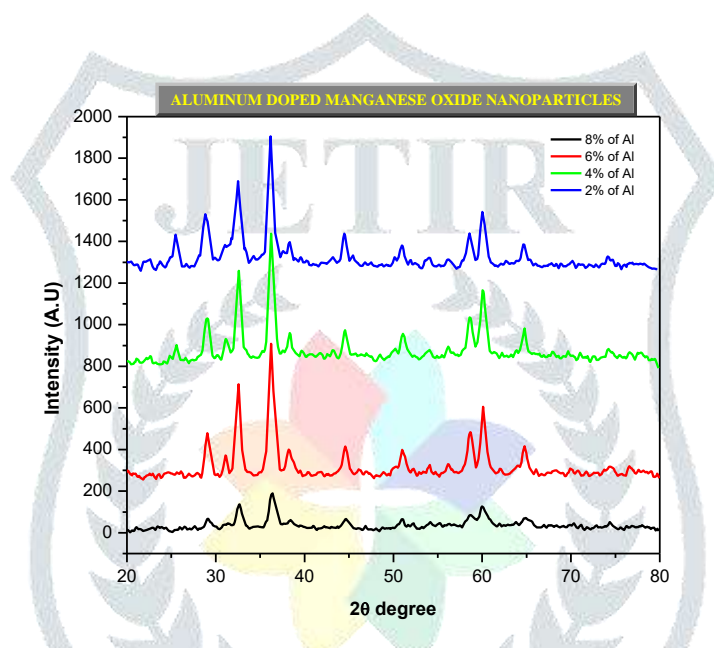


Fig 1 XRD pattern of Al doped Mn<sub>3</sub>O<sub>4</sub> nanoparticles

Table 1- Lattice parameters, crystallite size and strain from powder XRD pattern

sample	lattice parameters (Å)		crystallite size		unit cell volume (Å) <sup>3</sup>	strain X 10 <sup>-4</sup>
	a = b	c	(Debye Scherrer's) (nm)	(W-H plot) (nm)		
Mn <sub>3</sub> O <sub>4</sub> : Al (2%)	8.1168	9.3483	11.7456	16.718	615.88	20.1
Mn <sub>3</sub> O <sub>4</sub> : Al (4%)	8.1596	9.4059	15.1495	16.774	626.23	1.4631
Mn <sub>3</sub> O <sub>4</sub> : Al (6%)	8.1735	9.388	16.7721	17.666	627.18	-1.9861
Mn <sub>3</sub> O <sub>4</sub> : Al (8%)	8.1927	9.4892	17.5495	18.123	636.92	-11.5

From W-H plot the lower (2 and 4% Al) dopant concentration produce the positive slope shows that the strain is tensile in nature. But for higher dopant concentration exhibit negative slope represents the flexibility. By linear fit, y-intercept gives inverse of particle size and strain are calculated from the slope. Lattice parameters, crystallite thickness from Debye Scherrer's and W-H plot, strain are reported in Table 1. The thickness of the sample slightly increases with dopant concentration increases. Ionic radius for Mn<sup>2+</sup> 97 Å and Al<sup>3+</sup> 67.5 Å; Al<sup>3+</sup> ions well incorporated to Mn<sup>2+</sup> ions.

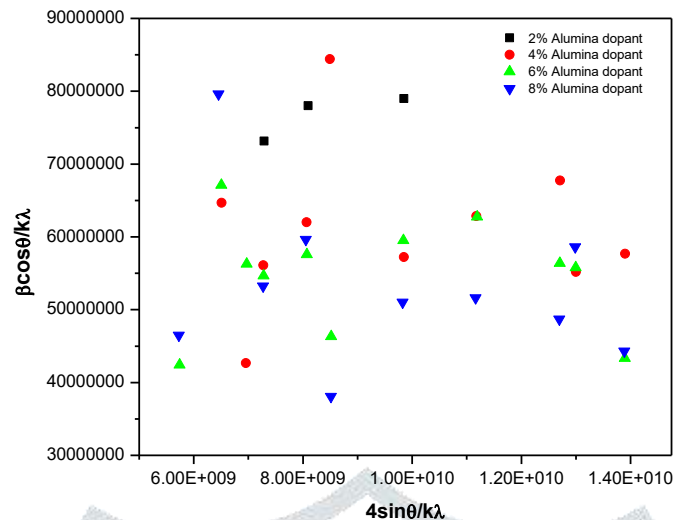


Fig 2 W-H plot for Al doped  $Mn_3O_4$  nanoparticles

### 3.2 Spectral analysis of Al doped $Mn_3O_4$ by FTIR analysis

The FTIR spectrum are used to classify the functional groups on the surface of as-synthesized Aluminum doped  $Mn_3O_4$  nanoparticles. Figure 3 denotes the FTIR spectrum of Al doped  $Mn_3O_4$  nanoparticles. The absorption peak near  $3312\text{ cm}^{-1}$  are flexible vibration of hydroxyl group on the surface of nanoparticles; it is wider and stronger in (2, 8% of Al) concentration of aluminum. For 4 and 6% of aluminum at  $3312\text{ cm}^{-1}$  diminished and exhibits the crystallinity of the samples [8]. The peak at  $1540\text{ cm}^{-1}$  represents O-H stretching vibrations on manganese atoms. The peak around  $500\text{--}600\text{ cm}^{-1}$  exhibits Mn-O stretching mode of vibration. The vibrational modes at  $637\text{ cm}^{-1}$  is assigned to the substitution of  $Al^{3+}$  for  $Mn^{2+}$  sites [9].

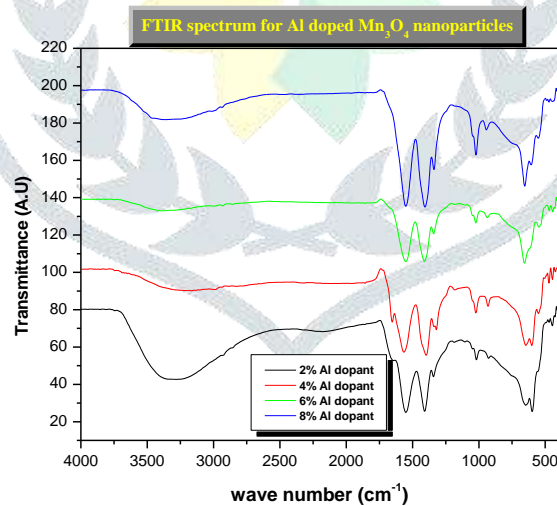


Fig 3 FTIR spectral analysis for Al doped  $Mn_3O_4$  nanoparticles

### 3.3 Morphological studies of Al doped $Mn_3O_4$

#### 3.3.1 Scanning electron microscope analysis (SEM):

The morphology of as-prepared Al (4 and 6%) doped  $Mn_3O_4$  nanoparticles was captured by SEM images, which are shown in Figure 4 (a) and (b). Low and high magnifications of SEM micrographs of as-prepared product is composed of aggregated spherical shaped nanoparticles.

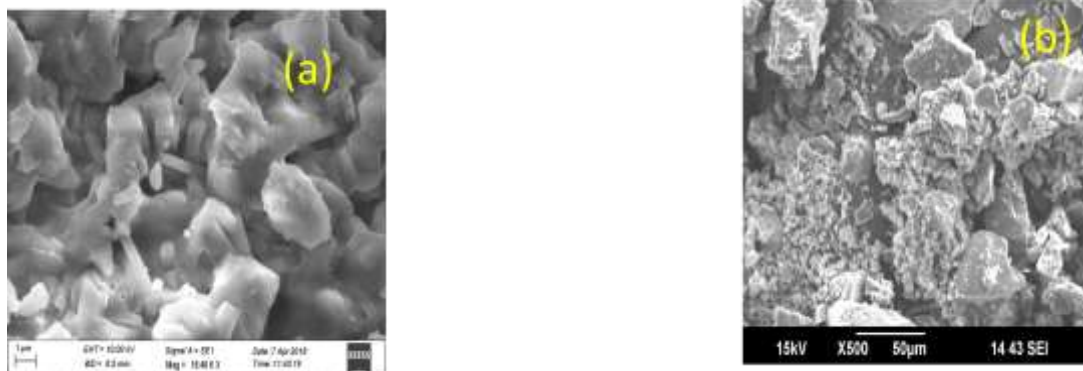


Fig 4 (a) and (b) SEM micrographs for Al (4 and 6%) doped  $Mn_3O_4$  nanoparticles

### 3.3.2 Field emission scanning electron microscope analysis (FESEM):

The particle size distribution of Al doped nanoparticles could be obtained by measuring the size of about 700 number of particles in FESEM image using the Image-J program. Figure 5 FESEM pictures for Al (2%) doped  $Mn_3O_4$  nanosystem for low and high magnification.

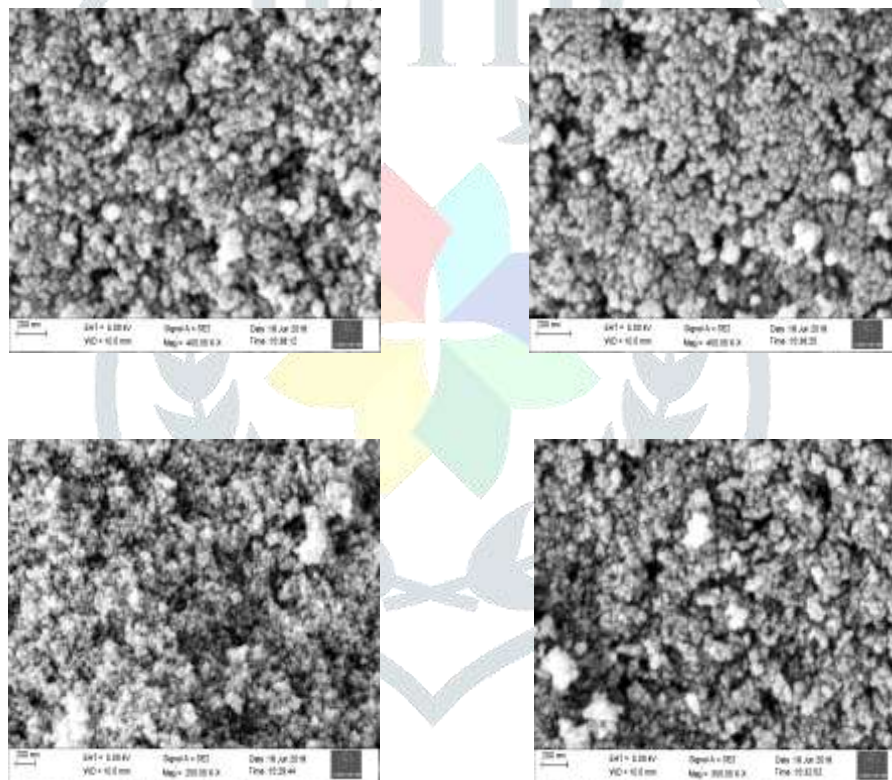


Fig 5 FESEM pictures for 2% Al doped  $Mn_3O_4$  nanoparticles for different magnification

### 3.3.3 Transmission electron microscope analysis (TEM):

The TEM images are used to get further information regarding the structural aspects of tetragonal Al doped  $Mn_3O_4$  spherical nanoparticles, which are in good agreement with FESEM observations. The SAED pattern reveals the aluminum doped  $Mn_3O_4$  nanoparticles are crystalline in nature. The size of the nanoparticles according to the TEM images was found to be below 20 nm. The SAED pattern of as-obtained nanoparticles as shown in the lower inset Figure 6.



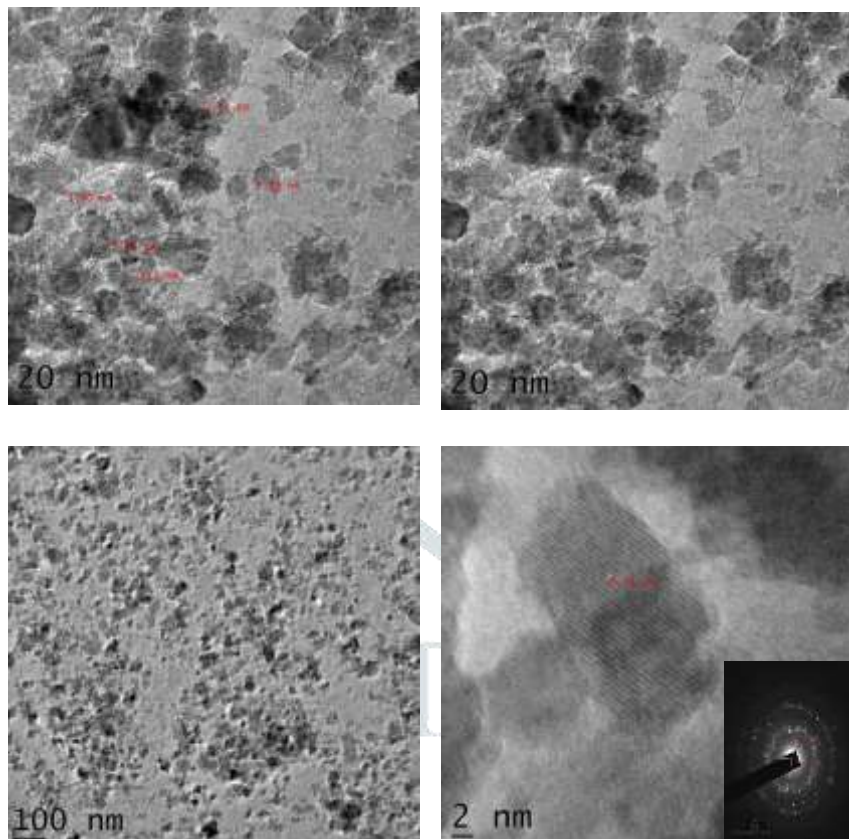


Fig 6 TEM images of as-prepared Al (8%) doped  $Mn_3O_4$  nanoparticles

### 3.4 Purity of the sample by EDAX spectral analysis

The chemical composition of the nanoparticles has been analyzed using EDAX analysis as shown in Fig.7.

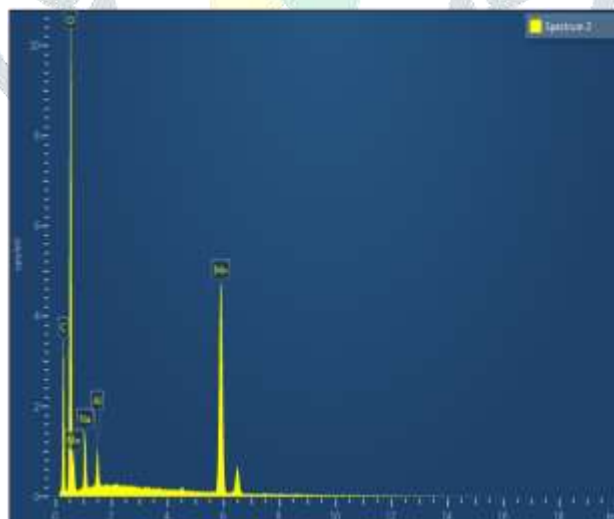


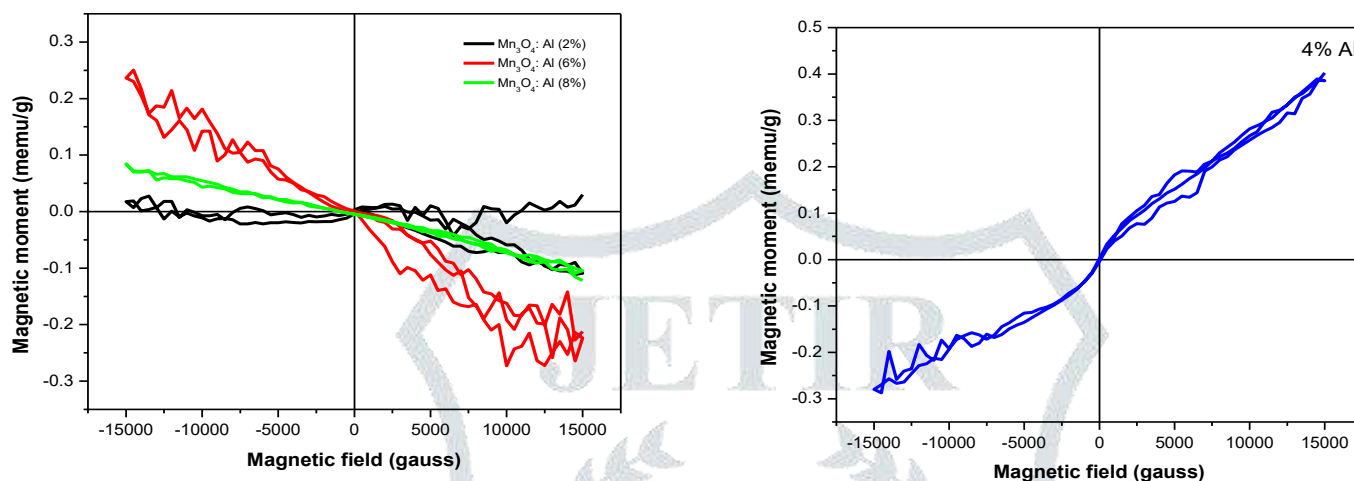
Fig 7 EDAX spectrum of Aluminum doped  $Mn_3O_4$  nanoparticles

### 3.5 Magnetic properties of Al doped $Mn_3O_4$ by VSM analysis:

Figure 8 show that the magnetic behavior of Al doped  $Mn_3O_4$  nanoparticles. The influence of diamagnetic material aluminum doped to the antiferromagnetic material manganese tetroxide behaved as superparamagnetic at room temperature [10]. The magnetic parameters observed from M-H curve presented in table 2. The thickness of the sample increases the magnetic parameters coercivity; retentivity and squareness ratio are decreases.

Table 2 Magnetic parameters of Al (2%, 4%, 6% and 8%) doped Mn<sub>3</sub>O<sub>4</sub> nanoparticles

sample	thickness (nm)	coercivity (gauss)	magnetization (μemu)	retentivity (μemu)	squareness ratio (M <sub>r</sub> /M <sub>s</sub> )
Mn <sub>3</sub> O <sub>4</sub> : Al (2%)	12	1823	704.62	35.910	0.05096
Mn <sub>3</sub> O <sub>4</sub> : Al (4%)	15	582.65	3448.1	33.069	0.00959
Mn <sub>3</sub> O <sub>4</sub> : Al (6%)	17	370.56	2877.7	15.269	0.005306
Mn <sub>3</sub> O <sub>4</sub> : Al (8%)	18	41.796	1546.2	7.3987	0.004785

Fig 8 M-H curves for Al (2%, 4%, 6% and 8%) doped Mn<sub>3</sub>O<sub>4</sub> nanoparticles

## CONCLUSION

Aluminum doped manganese tetroxide nanoparticles are successfully synthesized with a single phase exists. From the powder XRD results the crystallite size of the aluminum doped Mn<sub>3</sub>O<sub>4</sub> samples are below 20 nm and is confirmed by SEM, FESEM and TEM analysis. The crystallite size slightly increases with the dopant concentration increases. FTIR and EDAX results illustrate that purity of the samples. From the VSM analysis increasing the amount of aluminum, the coercivity and retentivity are decreases. The squareness ratio is very small but positive value. At (2%) low concentration of aluminum the magnetization value is very small and that is behave like a diamagnetic material. Addition of Al<sup>3+</sup> ions the material slowly gains the magnetic effect.

## References

1. Tierui Zhang, Qiao Zhang, Jianping Ge, James Goebel, Minwei Sun, Yushan Yan, Yi-sheng Liu, Chinglin Chang, Jinghua Guo and Yadong Yin, 2009, 'A Self-Templated Route to Hollow Silica Microspheres', *J. Phys. Chem. C*, 11 (8), 3168–3175.
2. Eftehari A, 2004, 'Aluminum oxide as a multifunction agent for improving battery performance of LiMn<sub>3</sub>O<sub>4</sub> cathode', *Solid State Ionics*, 167, 237-242.
3. Kim KW, Lee SW, Han KS et al., 2003, 'Characterization of Al-doped spinel LiMn<sub>2</sub>O<sub>4</sub> thin film cathode electrodes prepared by liquid source misted chemical deposition technique', *Journal of Electrochim Acta*, 48, 4223-4231.
4. Yu P, Zhang X, Wang DL, Wang L, Ma YW, 2009, 'Shape-controlled synthesis of 3D hierarchical MnO<sub>2</sub> nanostructures for electrochemical supercapacitors', *Cryst Growth Des* 9, 528-533.
5. Guiling Wang, Guangjie Shao, Lin Wang, Jianjun Song, Zhipeng Ma & Tingting Liu, 2014, "Enhanced electrochemical properties of Al doped bulk manganese oxides synthesized by a facile liquid-phase method", *Ionics*, 20 (10), 1367-1375.
6. Guiling Wang, Guangjie Shao, Jianping Du, Ying Zhang and Zhipeng Ma, 2013, 'Effect of doping cobalt on the micro-morphology and electrochemical properties of birnessite MnO<sub>2</sub>', *Materials Chemistry and Physics*, 138, 108-113.
7. Zhang Shu and Shulin Wang, 2009, 'Synthesis and Characterization of Magnetic Nanosized Fe<sub>3</sub>O<sub>4</sub>/MnO<sub>2</sub> Composite Particles', *Journal of Nanomaterials*, 2009, 1-5.
8. Gomaa A.M. Ali, Ling Ling Tan, Rajan Jose, Mashitah M. Yusoff, 2014, 'Electrochemical performance studies of MnO<sub>2</sub> nanoflowers recovered from spent battery', *Materials research Bulletin*, 60, 5-9.
9. Simona cavalu & Florin Banica, 2013, 'Surface modification of Alumina/Zirconia ceramics upon different fluoride -Based treatments', *International journal of applied ceramics*, 1-10.
10. Arab Mohammad Toufiq, Fengping Wang, Qurat-ul-ain Javed, Quanshui Li, Yan Li, 2014, 'Hydrothermal synthesis of MnO<sub>2</sub> nanowires: structural characterizations, optical and magnetic properties', *Appl. phys. A*, 116, 1127-1132.